JACS ARTICLES

Published on Web 06/03/2009

Stereospecific Formation of the (*R*)-γ-Hydroxytrimethylene Interstrand N^2-dG:N^2-dG Cross-Link Arising from the γ-OH-1,N^2-Propano-2′-deoxyguanosine Adduct in the 5′-CpG-3′ DNA Sequence

Hai Huang, Hye-Young Kim, Ivan D. Kozekov, Young-Jin Cho, Hao Wang, Albena Kozekova, Thomas M. Harris, Carmelo J. Rizzo, and Michael P. Stone*

Department of Chemistry and Center in Molecular Toxicology, Vanderbilt University, Nashville, Tennessee 37235

Received December 6, 2008; E-mail: michael.p.stone@vanderbilt.edu

Abstract: Acrolein reacts with dG to form hydroxylated 1,N^2-propanodeoxyguanosine (OH-PdG) adducts. Most abundant are the epimeric 3-(2-deoxy-β-D-*erythro*-pentofuranosyl)-5,6,7,8-tetrahydro-8-hydroxypyrimido[1,2*a*] purin-10(3*H*)-ones, commonly referred to as the γ-OH-PdG adducts. When placed complementary to deoxycytosine in duplex DNA, these undergo rearrangement to the N^2-(3-oxopropyl)-dG aldehyde. The latter forms diastereomeric interstrand N^2-dG:N^2-dG cross-links in the 5′-CpG-3′ sequence. Here we report the structure of the stereochemically favored (*R*)-γ-hydroxytrimethylene N^2-dG:N^2-dG interstrand DNA cross-link in 5′-d($G^1C^2T^3A^4G^5C^6X^7A^8G^9T^{10}C^{11}C^{12}$)-3′·5′-d($G^{13}G^{14}A^{15}C^{16}T^{17}C^{18}Y^{19}C^{20}T^{21}A^{22}G^{23}C^{24}$)-3′ ($X^7$ is the dG linked to the α-carbon of the carbinolamine linkage, and Y^{19} is the dG linked to the γ-carbon of the carbinolamine linkage; the cross-link is in the 5′-CpG-3′ sequence). The structure was characterized using isotope-edited ^{15}N nuclear Overhauser enhancement spectroscopy heteronuclear single quantum correlation (NOESY-HSQC) NMR, in which the exocyclic amines at X^7 or Y^{19} were ^{15}N-labeled. Analyses of NOE intensities involving Y^{19} N^2H indicated that the (*R*)-γ-hydroxytrimethylene linkage was the major cross-link species, constituting 80−90% of the cross-link. The X^7 and Y^{19} imino resonances were observed at 65 °C. Additionally, for the 5′-neighbor base pair G^5·C^{20}, the G^5 imino resonance remained sharp at 55 °C but broadened at 65 °C. In contrast, for the 3′-neighbor A^8·T^{17} base pair, the T^{17} imino resonance was severely broadened at 55 °C. Structural refinement using NOE distance restraints obtained from isotope-edited ^{15}N NOESY-HSQC data indicated that the (*R*)-γ-hydroxytrimethylene linkage maintained the C^6·Y^{19} and X^7·C^{18} base pairs with minimal structural perturbations. The (*R*)-γ-hydroxytrimethylene linkage was located in the minor groove. The X^7 N^2 and Y^{19} N^2 atoms were in the gauche conformation with respect to the linkage, which maintained Watson−Crick hydrogen bonding of the cross-linked base pairs. The anti conformation of the hydroxyl group with respect to C^α of the tether minimized steric interaction and, more importantly, allowed the formation of a hydrogen bond between the hydroxyl group and C^{20} O^2 located in the 5′-neighboring base pair G^5·C^{20}. The formation of this hydrogen bond may, in part, explain the thermal stability of this carbinolamine interstrand cross-link and the stereochemical preference for the (*R*) configuration of the cross-link.

Introduction

DNA interstrand cross-links represent a severe form of DNA damage due to their ability to block DNA replication and transcription.[1,2] The nucleotide excision repair (NER) pathway is involved in the repair of the interstrand cross-link lesion.[3] Many chemicals cause interstrand cross-links, including bifunctional alkylating agents, platinum compounds, and psoralen.[3] α,β-Unsaturated aldehydes (enals) such as acrolein,[4−6] crotonaldehyde,[5] and *trans*-4-hydoxynonenal (HNE)[7] represent a group of chemicals that produce DNA interstrand cross-links. They are produced from the incomplete combustion of organic matter such as fuels, wood, and tobacco;[8,9] enals are also produced endogenously as a byproduct of lipid peroxidation.[10−17]

Enals are mutagenic.[18−22] They are bis-electrophiles and undergo sequential reaction with two nucleophilic groups of DNA bases. Reaction of deoxyguanosine with enals produce exocyclic 1,N^2-deoxyguanosine adduct **1** through an initial Michael addition.[23−27] When placed opposite deoxycytosine in

(1) Lawley, P. D.; Brookes, P. *Nature* **1965**, *206*, 480–483.
(2) Lawley, P. D.; Brookes, P. *J. Mol. Biol.* **1967**, *25*, 143–160.
(3) Noll, D. M.; Mason, T. M.; Miller, P. S. *Chem. Rev.* **2006**, *106*, 277–301.
(4) Kozekov, I. D.; Nechev, L. V.; Sanchez, A.; Harris, C. M.; Lloyd, R. S.; Harris, T. M. *Chem. Res. Toxicol.* **2001**, *14*, 1482–1485.
(5) Kozekov, I. D.; Nechev, L. V.; Moseley, M. S.; Harris, C. M.; Rizzo, C. J.; Stone, M. P.; Harris, T. M. *J. Am. Chem. Soc.* **2003**, *125*, 50–61.
(6) Sanchez, A. M.; Kozekov, I. D.; Harris, T. M.; Lloyd, R. S. *Chem. Res. Toxicol.* **2005**, *18*, 1683–1690.
(7) Wang, H.; Kozekov, I. D.; Harris, T. M.; Rizzo, C. J. *J. Am. Chem. Soc.* **2003**, *125*, 5687–5700.
(8) Witz, G. *Free Radical Biol. Med.* **1989**, *7*, 333–349.
(9) Stevens, J. F.; Maier, C. S. *Mol. Nutr. Food Res.* **2008**, *52*, 7–25.
(10) Pan, J.; Chung, F. L. *Chem. Res. Toxicol.* **2002**, *15*, 367–372.

10.1021/ja809543j CCC: $40.75

duplex DNA, these exocyclic 1,N^2-dG adducts undergo ring-opening to N^2-(3-oxopropyl) adduct **2**, unveiling a reactive aldehyde functionality; it exists in equilibrium with the corresponding aldehydrols **3** or related species (Scheme 1).[28−31] We have demonstrated that the N^2-amino group of a neighboring deoxyguanosine on the complementary strand can react with the ring-opened aldehyde to form an interstrand N^2-dG:N^2-dG cross-link.[4−7,32]

The formation of the DNA interstrand cross-links by the exocyclic 1,N^2-deoxyguanosine adducts is sequence-dependent, occurring in the local 5′-CpG-3′ sequence context but not in the 5′-GpC-3′ sequence context.[5] This is attributed to the longer distance between the N^2-dG atoms in the 3′-direction than in the 5′-direction. The formation of a three-carbon tether in the 3′-direction greatly perturbs the cross-linked base pairs and destabilizes the DNA duplex.[33,34] The formation of interstrand cross-links is also influenced by the stereochemistry of the exocyclic 1,N^2-dG adducts derived from enals with longer carbon chains.[5,7] The crotonaldehyde-derived 1,N^2-deoxyguanosine adduct of (6*R*) configuration induces interstrand cross-linking more efficiently than does the (6*S*) diastereomer.[5] Structure and modeling studies reveal that the orientations of the aldehyde group in the ring-opened (*R*)- and (*S*)-crotonaldehyde-derived 1,N^2-dG adducts are different.[28] Steric interactions between the methyl group of the cross-link of the (6*S*) diastereomer with the neighboring base pairs result in perturbations of the DNA duplex;[28,35] these unfavorable steric interactions are not present in the (6*R*) cross-link. Similar considerations apply to the HNE-derived 1,N^2-dG adducts,[36] of which only the (6*S*,8*R*,11*S*) configuration forms interstrand cross-links in the 5′-CpG-3′ sequence.[7]

Scheme 1. Chemistry of an Enal-Derived Exocyclic 1,N^2-Deoxyguanosine Adduct in the 5′-CpG-3′ Sequence When Placed Opposite Deoxycytosine in Duplex DNA

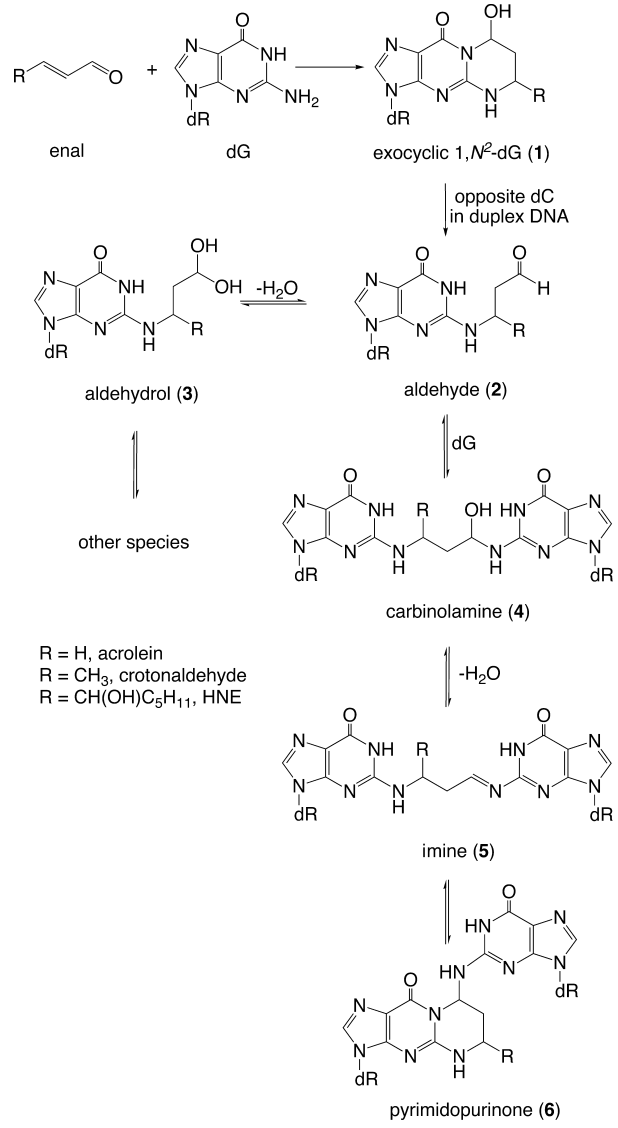

Possible structures for the DNA interstrand cross-links include carbinolamine **4**, imine **5**, and the ring-closed pyrimidopurinone **6**, or possibly an equilibrium mixture of all three (Scheme 1). Pyrimidopurinone **6** is observed upon enzymatic digestion of the cross-linked DNA duplex[5,7] but is undetectable in the duplex oligodeoxynucleotides.[28,29,37] Although the existence of imine **5** in duplex DNA is surmised by the observation that the

(11) Chung, F. L.; Nath, R. G.; Nagao, M.; Nishikawa, A.; Zhou, G.-D.; Randerath, K. *Mutat. Res.* **1999**, *424*, 71–81.
(12) Wilson, V. L.; Foiles, P. G.; Chung, F. L.; Povey, A. C.; Frank, A. A.; Harris, C. C. *Carcinogenesis* **1991**, *12*, 1483–1490.
(13) Nath, R. G.; Ocando, J. E.; Chung, F. L. *Cancer Res.* **1996**, *56*, 452–456.
(14) Nath, R. G.; Chung, F.-L. *Proc. Natl. Acad. Sci. U.S.A.* **1994**, *91*, 7491–7495.
(15) Benedetti, A.; Comporti, M.; Esterbauer, H. *Biochim. Biophys. Acta* **1980**, *620*, 281–296.
(16) Esterbauer, H.; Schaur, R. J.; Zollner, H. *Free Radical Biol. Med.* **1991**, *11*, 81–128.
(17) Burcham, P. C. *Mutagenesis* **1998**, *13*, 287–305.
(18) Sierra, L. M.; Barros, A. R.; García, M.; Ferreiro, J. A.; Comendador, M. A. *Mutat. Res.* **1991**, *260*, 247–256.
(19) Yang, I. Y.; Johnson, F.; Grollman, A. P.; Moriya, M. *Chem. Res. Toxicol.* **2002**, *15*, 160–164.
(20) Czerny, C.; Eder, E.; Rünger, T. M. *Mutat. Res.* **1998**, *407*, 125–134.
(21) Jha, A. M.; Singh, A. C.; Sinha, U.; Kumar, M. *Mutat. Res.* **2007**, *632*, 69–77.
(22) Eckl, P. M. *Mol. Aspects Med.* **2003**, *24*, 161–165.
(23) Chung, F.-L.; Young, R.; Hecht, S. S. *Cancer Res.* **1984**, *44*, 990–995.
(24) Gölzer, P.; Janzowski, C.; Pool-Zobel, B. L.; Eisenbrand, G. *Chem. Res. Toxicol.* **1996**, *9*, 1207–1213.
(25) Chung, F. L.; Young, R.; Hecht, S. S. *Carcinogenesis* **1989**, *10*, 1291–1297.
(26) Chung, F. L.; Chen, H. J.; Nath, R. G. *Carcinogenesis* **1996**, *17*, 2105–2111.
(27) Chung, F. L.; Nath, R. G.; Ocando, J.; Nishikawa, A.; Zhang, L. *Cancer Res.* **2000**, *60*, 1507–1511.
(28) Cho, Y.-J.; Wang, H.; Kozekov, I. D.; Kurtz, A. J.; Jacob, J.; Voehler, M.; Smith, J.; Harris, T. M.; Lloyd, R. S.; Rizzo, C. J.; Stone, M. P. *Chem. Res. Toxicol.* **2006**, *19*, 195–208.
(29) Cho, Y.-J.; Kim, H.-Y.; Huang, H.; Slutsky, A.; Minko, I. G.; Wang, H.; Nechev, L. V.; Kozekov, I. D.; Kozekova, A.; Tamura, P.; Jacob, J.; Voehler, M.; Harris, T. M.; Lloyd, R. S.; Rizzo, C. J.; Stone, M. P. *J. Am. Chem. Soc.* **2005**, *127*, 17686–17696.
(30) De los Santos, C.; Zaliznyak, T.; Johnson, F. *J. Biol. Chem.* **2001**, *276*, 9077–9082.
(31) Huang, H.; Wang, H.; Qi, N.; Kozekova, A.; Rizzo, C. J.; Stone, M. P. *J. Am. Chem. Soc.* **2008**, *130*, 10898–10906.
(32) Stone, M. P.; Cho, Y. J.; Huang, H.; Kim, H. Y.; Kozekov, I. D.; Kozekova, A.; Wang, H.; Minko, I. G.; Lloyd, R. S.; Harris, T. M.; Rizzo, C. J. *Acc. Chem. Res.* **2009**, *41*, 793–804.
(33) Dooley, P. A.; Zhang, M.; Korbel, G. A.; Nechev, L. V.; Harris, C. M.; Stone, M. P.; Harris, T. M. *J. Am. Chem. Soc.* **2003**, *125*, 62–72.
(34) Dooley, P. A.; Tsarouhtsis, D.; Korbel, G. A.; Nechev, L. V.; Shearer, J.; Zegar, I. S.; Harris, C. M.; Stone, M. P.; Harris, T. M. *J. Am. Chem. Soc.* **2001**, *123*, 1730–1739.
(35) Cho, Y. J.; Kozekov, I. D.; Harris, T. M.; Rizzo, C. J.; Stone, M. P. *Biochemistry* **2007**, *46*, 2608–2621.
(36) Huang, H.; Wang, H.; Qi, N.; Lloyd, R. S.; Rizzo, C. J.; Stone, M. P. *Biochemistry* **2008**, *47*, 11457–11472.
(37) Kim, H. Y.; Voehler, M.; Harris, T. M.; Stone, M. P. *J. Am. Chem. Soc.* **2002**, *124*, 9324–9325.

Scheme 2. Numbering Scheme of the Oligodeoxynucleotides Containing the (*R*)-γ-Hydroxytrimethylene Interstrand Cross-Link in the 5′-CpG-3′ Sequence[a]

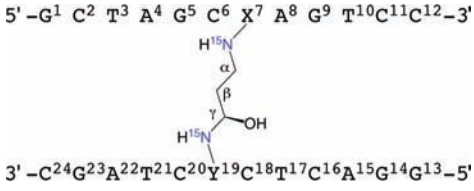

[a] The two ^{15}N isotopic labeling sites are indicated in blue.

interstrand cross-link can be reduced by $NaCNBH_3$,[5,7] the interstrand cross-links involving the acrolein- and crotonaldehyde-derived 1,N^2-dG adducts exist primarily as diastereomeric γ-hydroxytrimethylene (carbinolamine **4**) tethers at N^2-dG:N^2-dG positions (Scheme 2).[28,29,37] Both imine **2** or pyrimidopurinone **3** are predicted to perturb the Watson−Crick hydrogen bonding and stacking of the cross-linked base pairs, whereas the formation of the carbinolamine linkage has a minimum impact.[28,29]

Although structures of reduced models of these cross-links, in which a trimethylene chain links the N^2-positions, have been reported,[33,34] the native diastereomeric carbinolamine cross-links have not been examined. The observation of thermally stable carbinolamine interstrand cross-links in duplex DNA in aqueous solution[28,29] suggests that additional interactions might stabilize the linkage. Presently, we show that the acrolein-derived diastereomeric (*R*)-γ-hydroxytrimethylene N^2-dG:N^2-dG interstrand DNA cross-link is favored in 5′-d($G^1C^2T^3A^4G^5C^6X^7A^8$-$G^9T^{10}C^{11}C^{12}$)-3′•5′-d($G^{13}G^{14}A^{15}C^{16}T^{17}C^{18}Y^{19}C^{20}T^{21}A^{22}G^{23}C^{24}$)-3′ ($X^7$ is the dG linked to the α-carbon of the carbinolamine linkage, and Y^{19} is the dG linked to the γ-carbon of the carbinolamine linkage; the cross-link is in the 5′-CpG-3′ sequence). The structure has been characterized using isotope-edited ^{15}N nuclear Overhauser enhancement spectroscopy heteronuclear single quantum correlation (NOESY-HSQC) NMR. Analyses of NOE intensities involving the ^{15}N-labeled Y^{19} N^2H indicate that the (*R*)-γ-hydroxytrimethylene linkage is the major interstrand cross-link species, constituting 80−90% of the total cross-link. Structural refinement using NOE distance restraints obtained from isotope-edited ^{15}N NOESY-HSQC data indicates that the (*R*)-γ-hydroxytrimethylene linkage maintains the C^6•Y^{19} and X^7•C^{18} base pairs with minimal structural perturbations. The X^7 N^2 and Y^{19} N^2 atoms are in the gauche conformation with respect to the linkage, which maintains Watson−Crick hydrogen bonding of the cross-linked base pairs. The anti conformation of the hydroxyl group with respect to C^α of the tether minimizes steric interactions and allows the formation of a hydrogen bond between the hydroxyl group and C^{20} O^2 located in the 5′-neighboring base pair G^5•C^{20}. The formation of this hydrogen bond may, in part, explain the thermal stability of this carbinolamine interstrand cross-link and the stereochemical preference for the (*R*) configuration of the cross-link.

Results

Stereochemistry of the Carbinolamine Cross-Link. The carbinolamine interstrand cross-links of the acrolein adduct of dG were prepared as reported[5] and occurred as a mixture of (*R*) and (*S*) diastereomers at the carbinolamine carbon. An expansion of ^{15}N HSQC filtered NOESY spectrum of the Y^{19} N^2 ^{15}N-labeled interstrand cross-link is shown in Figure 1A. For the major diastereomeric cross-linked species, a complete set of NOEs between Y^{19} N^2H and the γ-hydroxytrimethylene tether was observed. The Y^{19} N^2H → H^γ NOE was weaker than the Y^{19} N^2H → $H^{\beta2}$ NOE and only slightly stronger than the two diastereotopic Y^{19} N^2H → H^α NOEs. This was consistent with modeling, in which the (*R*)-γ-hydroxytrimethylene tether placed Y^{19} N^2H and H^γ at a distance of 2.9−3.1 Å. In contrast, the modeling suggested that the (*S*)-γ-hydroxytrimethylene tether placed Y^{19} N^2H and H^γ at a closer distance of 2.2−2.4 Å, which would have resulted in a stronger NOE. In addition, a weak Y^{19} H1′ → H^γ NOE was observed (Figure 1B), suggesting H^γ was oriented toward Y^{19}. These data indicated that the (*R*)-γ-hydroxytrimethylene linkage (Scheme 2) was the major interstrand cross-link species. The relative peak intensities in the ^{15}N HSQC spectrum suggested that the (*R*)-γ-hydroxytrimethylene cross-link constituted 80−90% of the overall interstrand cross-links.

Spectral Assignments of the (*R*)-γ-Hydroxytrimethylene Cross-Link. By comparison of the nonisotope-edited NOESY spectrum with the ^{15}N NOESY-HSQC spectrum of the X^7 N^2 ^{15}N-labeled interstrand cross-link, the G^5, X^7, T^{17}, and Y^{19} imino protons were assigned (Figure 2). The G^5 N1H → C^{20} N^4Hs, X^7 N1H → C^{18} N^4Hs, T^{17} N3H → A^8 H2, and Y^{19} N1H → C^6 N^4Hs NOE interactions arising from Watson−Crick hydrogen bonding were observed, indicating the Watson−Crick hydrogen bonds at the cross-linked base pairs were not significantly perturbed.

The base aromatic protons and the deoxyribose H1′ protons were assigned by comparing nonisotopically edited NOESY spectra of the modified duplex before and after cross-linking (Figure 3). For the freshly prepared duplex, aldehydrol **3** was the predominant species present in neutral solution.[29,30] The major NOE cross peaks in Figure 3, parts A and B, which were sequentially connected,[38,39] were therefore assigned to the correlations of aromatic H6/H8 protons with H1′ protons of aldehydrol **3**. The sample was then incubated for a week at 37 °C, during which time the interstrand cross-link **4** was formed and was eventually present for 50% of the duplexes[5,29] with the (*R*)-γ-hydroxytrimethylene predominant. Parts C and D of Figure 3 display the same region of the NOESY spectrum of the cross-linked sample. Except for the nucleotides close to the ends of the duplex, two sets of NOEs were sequentially assigned. The first set of NOEs were the same as those in Figure 3, parts A and B (not demonstrated in Figure 3, parts C and D) and arose from aldehydrol **3**, whereas the second set of NOEs were assigned to the (*R*)-γ-hydroxytrimethylene of cross-link **4**. These NOEs arising from cross-link **4** were sequentially connected with interruptions from C^6 to X^7 and from C^{18} to Y^{19} (Figure 3, parts C and D), indicating the (*R*)-γ-hydroxytrimethylene interstrand cross-link maintained a B-DNA geometry. The X^7 H8 → C^6 H1′ and Y^{19} H8 → C^{18} H1′ correlations were missing, and the A^8 H8 → X^7 H1′ interaction was stronger than other purine H8 → 5′-neighbor H1′ NOEs, indicating structural perturbation at the cross-linked base pairs. The assignments were supported by other NOEs such as H6/H8 → H3′, H6/H8 → H2′(′), H1′ → H3′, and H1′ → H2′(′), etc.

Stabilities of the Base Pairs for the (*R*)-γ-Hydroxytrimethylene Interstrand Cross-Link. The resonances of pyrimidine N3H and purine N1H imino protons at different temperatures are shown in Figure 4. The melting temperature (T_m) of the DNA interstrand cross-links was 91 °C in 1.0 M NaCl buffer.[5] The X^7 and Y^{19} imino resonances were still observable at 65

(38) Patel, D. J.; Shapiro, L.; Hare, D. *Q. Rev. Biophys.* **1987**, *20*, 35–112.
(39) Reid, B. R. *Q. Rev. Biophys.* **1987**, *20*, 2–28.

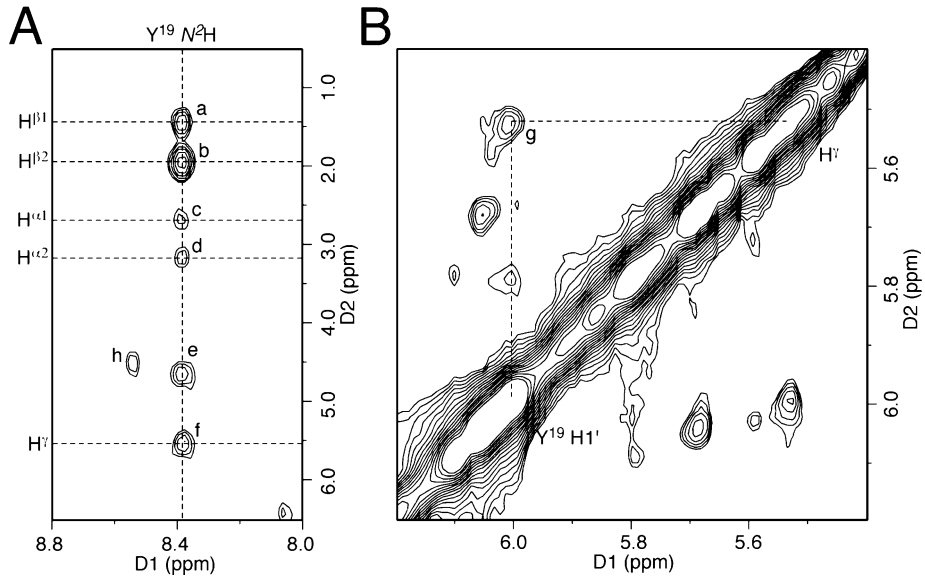

Figure 1. NOE cross peaks identifying the stereochemistry of the DNA interstrand cross-link. (A) ^{15}N NOESY-HSQC of the Y^{19} N^2 ^{15}N-labeled sample. (B) Nonisotope-edited NOESY. NOEs for the major diastereomer of the cross-link were assigned as (a) Y^{19} N^2H → $H^{\beta 1}$; (b) Y^{19} N^2H → $H^{\beta 2}$; (c) Y^{19} N^2H → $H^{\alpha 1}$; (d) Y^{19} N^2H → $H^{\alpha 2}$; (e) water exchange peak of Y^{19} N^2H; (f) Y^{19} N^2H → H^{γ}; (g) Y^{19} H1′ → H^{γ}; (h) Y^{19} N^2H → H^{γ} of the minor diastereomer.

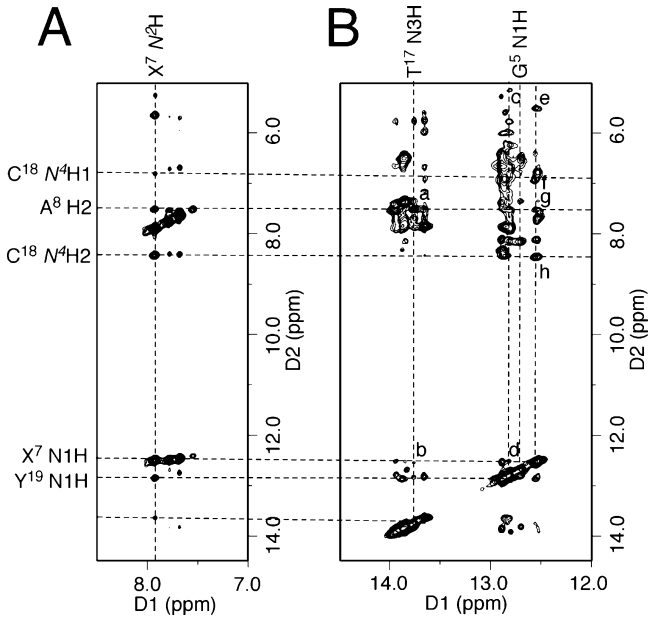

Figure 2. Expansions of NOESY spectra indicating G^5•C^{20}, C^6•Y^{19}, X^7•C^{18}, and A^8•T^{17} base pairs of the (*R*)-γ-hydroxytrimethylene cross-link maintained Watson−Crick base pairing. (A) ^{15}N NOESY-HSQC of the X^7 N^2 ^{15}N-labeled sample. (B) The nonisotopically edited NOESY spectrum. NOEs were assigned as (a) T^{17} N3H → A^8 H2; (b) T^{17} N3H → X^7 N1H; (c) Y^{19} N1H → C^6 H5; (d) Y^{19} N1H → X^7 N1H; (e) X^7 N1H → C^{18} H5; (f) X^7 N1H → C^{18} N^4H1; (g) X^7 N1H → A^8 H2; (h) X^7 N1H → C^{18} N^4H2.

°C, although starting to broaden, indicating the cross-linked base pairs were stabilized; this observation is consistent with a high-melting structure. For the 5′-neighbor base pair G^5•C^{20}, the G^5 imino resonance remained sharp at 55 °C but was broadened at 65 °C. At the 3′-neighbor A^8•T^{17} base pair, the T^{17} imino resonance was severely broadened at 55 °C. For the corresponding unmodified duplex these imino resonances were all broadened at 40 °C.

Chemical Shift Perturbations of the (*R*)-γ-Hydroxytrimethylene Cross-Link. The chemical shifts were compared with the corresponding unmodified duplex (Figure 5). Small chemical shift perturbations were observed for most of the nucleotides. The X^7•C^{18} base pair was minimally perturbed, and the C^{18} H6 and C^{18} H1′ resonances shifted upfield 0.11 and 0.32 ppm, respectively. The chemical shift perturbations for C^6•Y^{19} base pair were not remarkable. The C^6 H6, C^6 H1′, Y^{19} H8, and Y^{19} H1′ resonances shifted −0.03, −0.13, 0.06, and 0.09 ppm, respectively. Significantly, the 5′-neighboring C^{20} H6 had the most significant perturbation among the aromatic protons, 0.18 ppm downfield from the related proton in the unmodified sequence. C^{20} H5 and C^{20} H1′ also shifted downfield, 0.22 and 0.13 ppm, respectively, indicating the neighboring C^{20} was involved in the cross-link formation.

The backbone conformation was evaluated by the distribution of phosphorus resonances. The assignments of the C^6 and C^{18} H3′ protons of the cross-link were based upon their H1′ → H3′ and H6 → H3′ NOEs, respectively. They exhibited ^{31}P → H3′ correlations in the HMBC spectrum. In comparison with other nucleotides, the C^6 and C^{18} phosphates were shifted downfield, indicating that the backbone at the cross-linked base pairs was perturbed from ideal B-DNA.

Structural Refinement of the (*R*)-γ-Hydroxytrimethylene Cross-Link. The cross-link was simulated in explicit water at 300 K. The 19 NOE cross peaks in the ^{15}N NOESY-HSQC spectra assigned to X^7 N^2H and Y^{19} N^2H were converted to distance restraints to refine the cross-link tether. In addition, 52 empirical distance restraints and 200 empirical torsion angle restraints were used to maintain Watson−Crick hydrogen bonding and B-type DNA, respectively.

A fully solvated molecular dynamics simulation of 8 ns was carried out starting from both A- and B-type DNAs. The all-atom mass-weighted root-mean-square deviations (rmsd's) referenced to the starting structures were used to determine the time for the simulations to reach equilibrium and, in turn, the range of the trajectories to be used for the sequence analysis. The simulation equilibrated within 500−600 ps starting from A-type DNA and 200−300 ps starting from B-type DNA.

The rMD trajectories after simulating for 1 ns were used to analyze the potential hydrogen bonding of the carbinol hydroxyl group of the tether. Its occupancy by hydrogen bond acceptors

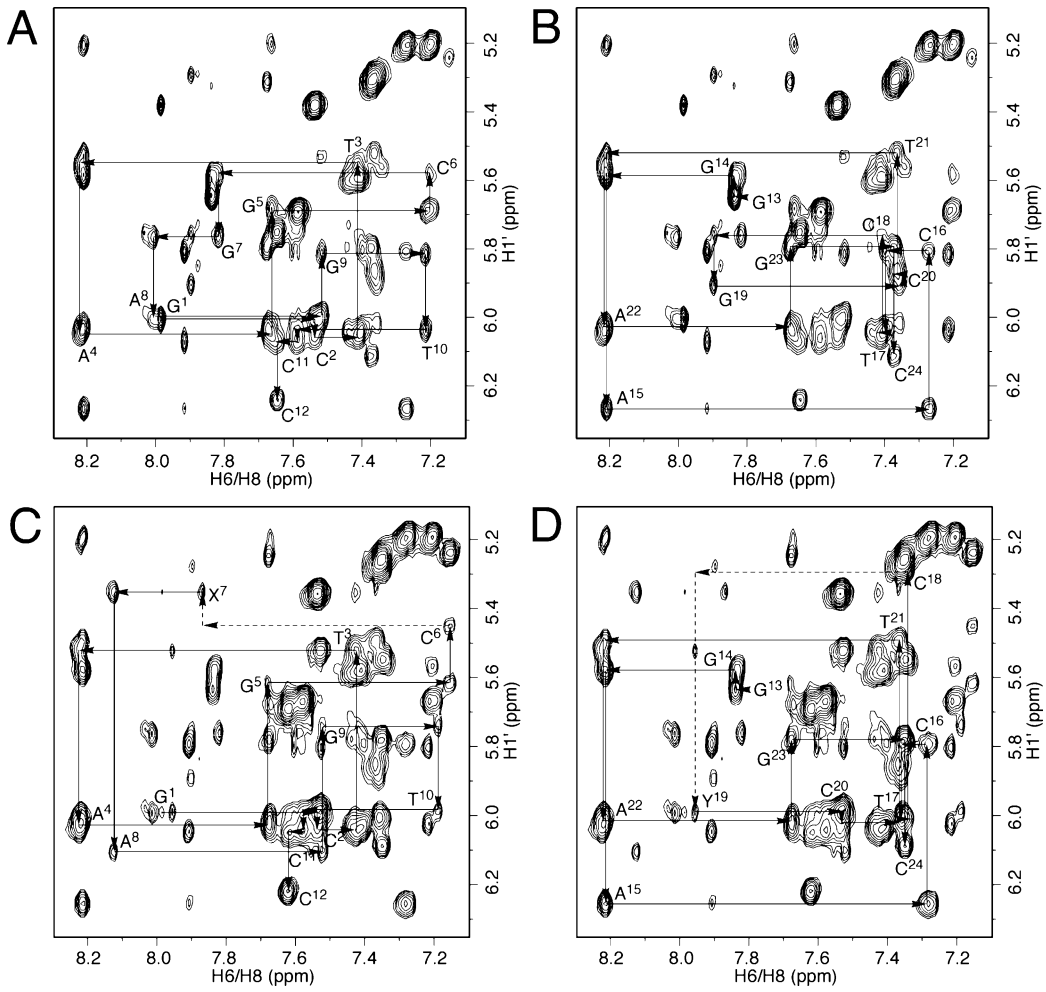

Figure 3. NOESY spectra of the duplex containing the acrolein-derived 1,N^2-dG exocyclic adduct and the resulting interstrand cross-links. (A and B) Duplex before cross-linking. The major NOEs, which were sequentially connected by solid lines, were assigned to the aldehydrol **3**. (C and D) Duplex after cross-linking. Two sets of NOE connectivities were assigned. One set arose from aldehydrol **3**, the other was assigned to (*R*)-γ-hydroxytrimethylene cross-link **4**. The NOEs of the (*R*)-γ-hydroxytrimethylene cross-link **4** were sequentially connected (solid and dashed lines). The X^7 H8 → C^6 H1′ and Y^{19} H8 → C^{18} H1′ NOEs were missing, and the A^8 H8 → X^7 H1′ correlation was stronger than corresponding others.

in the rMD trajectories revealed that it was likely to form a hydrogen bond in solution. Starting from both A- and B-type DNA, the simulations predicted the same hydrogen bond trends (Table 1). The carbinol hydroxyl group did not form a hydrogen bond with the solvent throughout the simulations. The duplex tended to adopt a conformation in which the hydroxyl group formed a hydrogen bond with C^{20} O^2, although the potential for a hydrogen bond to C^{20} O4′ was also observed. No hydrogen bonds with C^6 O^2 or Y^{19} N3 were formed.

The trajectories of the molecular dynamics simulations from 1 to 8 ns starting from A- and B-type DNAs were averaged. The rmsd value of these two refined structures was 0.54 Å, reflecting the similarities of the converged structures. The atom distances agreed with the NOE intensities and suggested that the refined structures obtained from the molecular dynamics simulations were accurate. Significantly, for the refined structures, the Y^{19} N^2H → H$^\gamma$ distance was 3.0 Å, which corroborated the observation of a weak NOE between Y^{19} N^2H and H$^\alpha$. The NOEs in Figure 3, parts C and D, were not used as the distance restraints. The distances of X^7 H8 → C^6 H1′, A^8 H8 → X^7 H1′, and Y^{19} H8 → C^{18} H1′ in the average structure were 6.0, 2.9, and 5.5 Å, respectively. Consistently, the X^7 H8 → C^6 H1′ and Y^{19} H8 → C^{18} H1′ NOEs were missing and A^8 H8 → X^7 H1′ NOE were stronger than other NOEs of aromatic protons with the 5′-neighbor H1′ protons (Figure 3, parts C and D). Other isolated NOEs of the cross-link in Figure 3, parts C and D, also agreed with the average structure. These indicated that the average structure provided an accurate depiction of the NMR data.

Refined Structure of the (*R*)-γ-Hydroxytrimethylene Cross-Link. Starting from either A- or B-type DNA, the cross-link converged to B-type with the tether located in the minor groove. Figure 6A provides an expanded view of the average structure observed from the minor groove. Consistent with Y^{19} N1H → C^6 N^4Hs and X^7 N1H → C^{18} N^4Hs NOEs (Figure 2), the C^6•Y^{19} and X^7•C^{18} base pairs conserved Watson−Crick hydrogen bonding with small distortions. They were closer to each other as compared to other base pairs. The backbone torsion angles of C^6, X^7, C^{18}, and Y^{19} were not ideal B-form geometry and agreed with the downfield shifts of C^6 and C^{18} phosphates.

The (*R*)-γ-hydroxytrimethylene tether was located in the minor groove (Figure 6A). The β-carbon oriented toward C^6 and X^7. Figure 7 provides Newman projections of the tether viewed along the C$^\alpha$−C$^\beta$ and C$^\beta$−C$^\gamma$ bonds. Both X^7 N^2 and Y^{19} N^2 were in the gauche conformation with respect to the (*R*)-γ-hydroxytrimethylene tether, which facilitated the Watson−Crick hydrogen bonding of the C^6•Y^{19} and X^7•C^{18} base pairs.

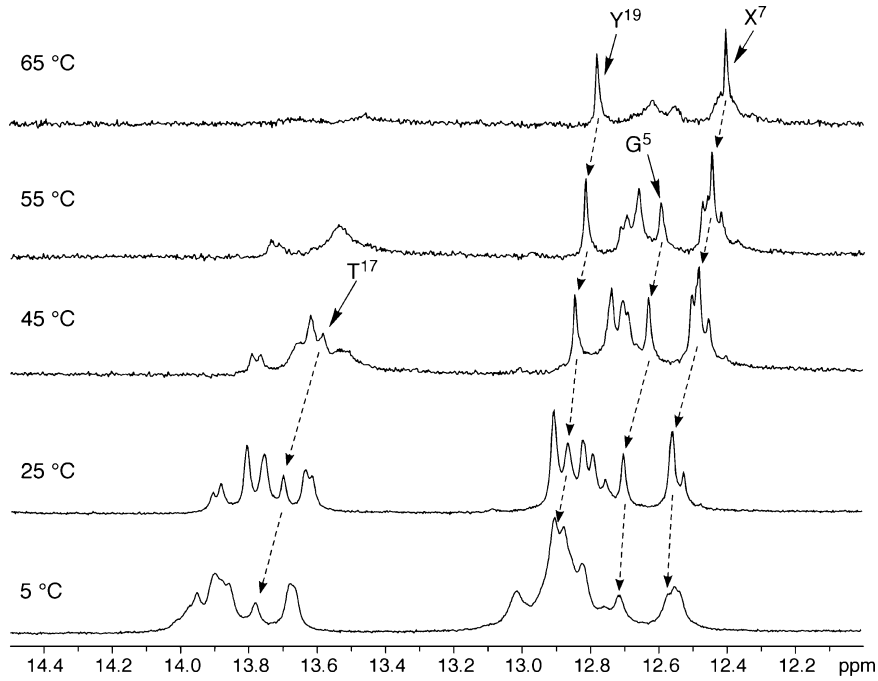

Figure 4. NMR melting studies of the (*R*)-γ-hydroxytrimethylene interstrand cross-link showing base pairs $G^5 \cdot C^{20}$, $C^6 \cdot Y^{19}$, and $X^7 \cdot C^{18}$ at the cross-linked region were stabilized.

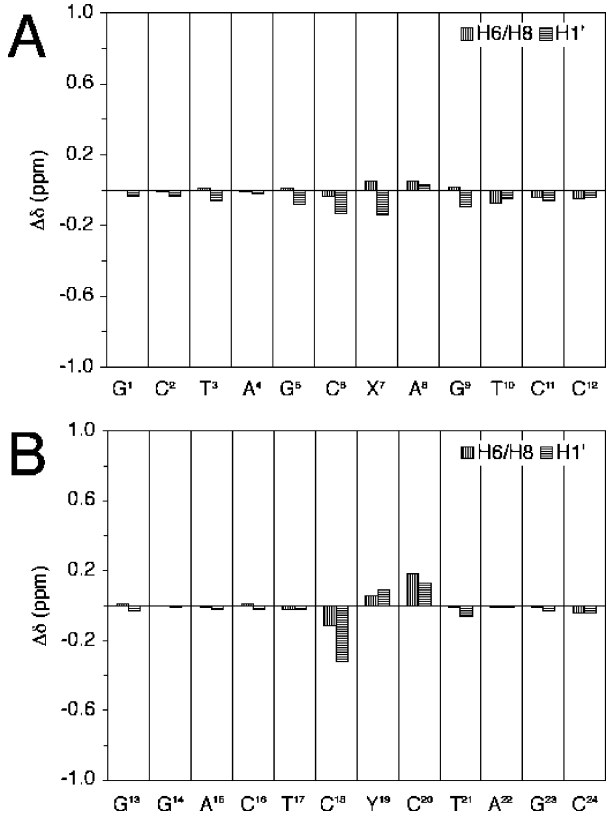

Figure 5. Chemical shift perturbations of the (*R*)-γ-hydroxytrimethylene interstrand cross-link compared to the unmodified duplex.

The trans configuration of the hydroxyl group with C^{α} minimized their steric interaction.

As shown in Figure 6A, the hydroxyl group of the (*R*)-γ-hydroxytrimethylene tether oriented toward C^{20} O^2 and formed a hydrogen bond. The distance and angle of the carbinol OH → C^{20} O^2 in the average structure were 2.1 Å and 177°, respectively (Table 1). No hydrogen bond interaction existed between the hydroxyl group and C^6 O^2, Y^{19} N3, or C^{20} O4′. The orientation of the hydroxyl group toward C^{20} O^2 agreed with its occupancy by the hydrogen bond acceptors in the trajectory analysis (Table 1). The hydrogen bond was also consistent with the NMR data. The $G^5 \cdot C^{20}$ base pair was stabilized by the cross-link (Figure 4). Chemical shift perturbations of C^{20} H5, H6, and H1′ were observed (Figure 5). In contrast, chemical shifts of the corresponding cytosine H5, H6, and H1′ protons in the interstrand cross-links bridged by either a trimethylene[34] or α-methyltrimethylene tether,[35] in which a hydrogen bond is not possible, underwent small perturbations.

Table 1. Occupancy of the Hydroxyl Group by the Hydrogen Bond Acceptors during Molecular Dynamics Simulations and the Distances and Angles of the Corresponding Atoms in the Average Structure of the (*R*)-γ-Hydroxytrimethylene Cross-Link

potential hydrogen bond	occupancy of OH (%)[a] from A-DNA	occupancy of OH (%)[a] from B-DNA	distance (Å)	angle (deg)
carbinol OH → C^{20} O^2	62	74	2.1	177
carbinol OH → C^{20} O4′	22	14	3.0	97
carbinol OH → Y^{19} N3	2.7	1.7	3.2	103
carbinol OH → C^6 O^2	1.0	0.70	3.6	93
carbinol OH → solvent	0.20	0		

[a] The criteria for a hydrogen bond formation: distance ≤3.5 Å and angle ≥120°.

Molecular Dynamics Simulations of the (*S*)-γ-Hydroxytrimethylene Tether. It was not possible to obtain NOE-based distance restraints for the (*S*)-γ-hydroxytrimethylene tether, which was present in solution at only low levels (Figure 1). Consequently, to explore the conformational possibilities for this diastereomer of the cross-link, nonrestrained molecular dynamics simulations were carried out in explicit solvent, starting from either A- or B-DNAs, respectively. Parts B and C of Figure 6 show expanded views of the refined structures starting from A- and B-type DNAs, respectively. In both cases, the (*S*)-γ-hydroxytrimethylene tether converged to similar

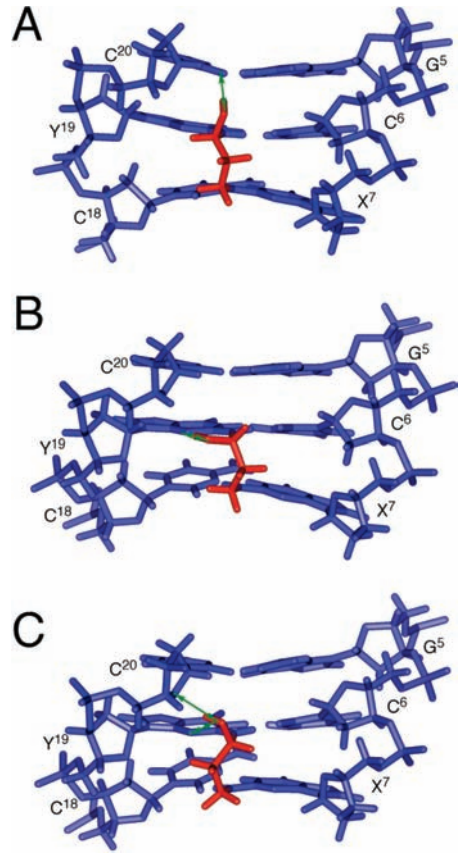

Figure 6. Expanded views, observed from the minor groove, of the diastereomeric carbinolamine interstrand cross-links. (A) Average structure of the (*R*)-γ-hydroxytrimethylene cross-link. (B) Predicted structure of the (*S*)-γ-hydroxytrimethylene cross-link from molecular dynamics simulations starting from A-DNA. (C) Predicted structure of the (*S*)-γ-hydroxytrimethylene cross-link from molecular dynamics simulations starting from B-DNA. Blue and red sticks represent nucleotides and the γ-hydroxytrimethylene tether, respectively. The green arrows indicate putative hydrogen bonds involving the hydroxyl groups.

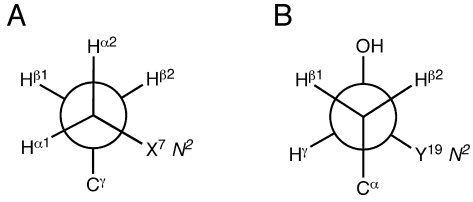

Figure 7. Newman projections showing conformation of the (*R*)-γ-hydroxytrimethylene tether. (A) Viewed along $C^{\alpha}-C^{\beta}$ bond. (B) Viewed along $C^{\beta}-C^{\gamma}$ bond. Both X^7 N^2 and Y^{19} N^2 were in the gauche conformation with the tether to maintain the Watson−Crick hydrogen bonding. The trans conformation of hydroxyl group with C^{α} minimizes the steric interaction and allows the formation of the carbinol OH → C^{20} O^2 hydrogen bond.

structures, but which were different from the refined structures of the (*R*)-γ-hydroxymethylene tether. For the (*S*)-γ-hydroxytrimethylene tether, the calculations predicted that the carbinol hydroxyl might form a hydrogen bond with Y^{19} N3 (Figure 6B) or a three-point hydrogen bond with Y^{19} N3 and C^{20} O4′ (Figure 6C). The distance for the Y^{19} N^2H to the H^{γ} for the (*S*)-γ-hydroxytrimethylene tether was 2.2 or 2.3 Å, respectively.

Discussion

Interstrand DNA cross-links block DNA replication and transcription, leading to cytotoxic and mutagenic effects if not repaired.[1,2] A DNA interstrand cross-link that covalently connects both strands represents a challenge for the cell, and an elaborate mechanism is required for its repair.[3] The DNA interstrand cross-link induced by the exocyclic 1,N^2-dG adduct **1** exists predominantly as carbinolamine **4** in equilibrium with imine **5** and pyrimidopurinone **6**. We have demonstrated that carbinolamine **4** is the only observable cross-linked species in duplex DNA.[29] Imine **5** and pyrimidopurinone **6** are predicted to cause significant perturbations to the DNA duplex and are thereby disfavored. Carbinolamine **4** might be anticipated to be readily reversible,[40−42] yet it stabilizes the DNA duplex with respect to thermal denaturation (T_m > 90 °C); thus, the forces involved in stabilizing these stereoisomeric carbinolamine interstrand cross-links are of interest.

(*R*)-γ-Hydroxytrimethylene Linkage as the Major Interstrand Cross-Link. The weak Y^{19} N^2H → H^{γ} and Y^{19} H1′ → H^{γ} NOE interactions (Figure 1) suggest that the (*R*)-γ-hydroxytrimethylene linkage is the major form of the interstrand cross-link. The (*R*)-γ-hydroxytrimethylene interstrand cross-link conserves B-type DNA geometry. The (*R*)-γ-hydroxytrimethylene tether has a minor groove orientation and adopts the U-conformation.[34] Watson−Crick hydrogen bonding of the cross-linked C^6•Y^{19} and X^7•C^{18} base pairs is conserved (Figure 6A). X^7 N^2 and Y^{19} N^2 are in the gauche orientation with respect to the α- or γ-carbons, respectively, in the extended chain conformation (Figure 7). The C^6•Y^{19} and X^7•C^{18} base pairs are placed closer as compared to others.

Role of Hydrogen Bonding in Interstrand Cross-Link Formation. The orientation of the (*R*)-γ-hydroxytrimethylene tether toward C^6 and X^7 minimizes the steric interaction of the bulky substituents (Figure 7) and facilitates the formation of a hydrogen bond between the hydroxyl group and C^{20} O^2 (Figure 6A), such as has been observed for type I aldolases in which the carbinolamine is stabilized in the active site.[43−46] Thermal denaturation of the DNA duplex results in the loss of this hydrogen bond, allowing the (*R*)-γ-hydroxytrimethylene tether to quickly dissociate.[5] The formation of this hydrogen bond to C^{20} O^2 augments the Watson−Crick hydrogen bonding (Figure 4) and base stacking of the cross-linked base pairs.

The presence of this hydrogen bond to C^{20} O^2 may, in part, explain the favored (*R*) stereochemistry of the carbinolamine linkage. These calculations suggested that, for the (*S*) stereochemistry, the hydroxyl group might form a hydrogen bond with Y^{19} N3 (Figure 6B) or a three-point hydrogen bond with Y^{19} N3 and C^{20} O4′ (Figure 6C), neither of which would be expected to stabilize the duplex in the same manner as the cross-link to C^{20} O^2. Overall, we suggest that formation of the carbinolamine linkage favors the (*R*) stereochemistry because in part of the favorable energetics associated with hydrogen bonding to C^{20} O^2.

(40) Jencks, W. P. *Catalysis in Chemistry and Enzymology*; McGraw-Hill: New York, 1969.
(41) Bruylants, A.; Feytmants-de Medicis, E. In *Chemistry of Carbon−Nitrogen Double Bonds*; Patai, S., Ed.; Interscience: London, 1970; pp 465−504.
(42) Bruckner, R. *Advanced Organic Chemistry: Reaction Mechanisms*; Harcourt/Academic Press: San Diego, CA, 2002.
(43) Allard, J.; Grochulski, P.; Sygusch, J. *Proc. Natl. Acad. Sci. U.S.A.* **2001**, *98*, 3679–3684.
(44) Erskine, P. T.; Newbold, R.; Brindley, A. A.; Wood, S. P.; Shoolingin-Jordan, P. M.; Warren, M. J.; Cooper, J. B. *J. Mol. Biol.* **2001**, *312*, 133–141.
(45) Thorell, S.; Schürmann, M.; Sprenger, G. A.; Schneider, G. *J. Mol. Biol.* **2002**, *319*, 161–171.
(46) Heine, A.; DeSantis, G.; Luz, J. G.; Mitchell, M.; Wong, C.-H.; Wilson, I. A. *Science* **2001**, *294*, 369–374.

Comparison to Reduced Trimethylene Cross-Links. We previously cross-linked DNA duplexes containing either the 5′-CpX-3′ or 5′-XpC-3′ sequence contexts with trimethylene tethers to simulate DNA interstrand cross-links induced by malondialdehyde and acrolein derived 1,N^2-dG adducts.[33,34] The preferential formation of the interstrand cross-link in the 5′-CpX-3′ sequence as compared to the 5′-XpC-3′ sequence was attributed to the greater destabilization of the DNA duplex by the cross-link in the 5′-XpC-3′ sequence, associated with greater structural distortion.[33,34] The accompanying structural refinements[33,34] indicated a greater perturbation of Watson−Crick hydrogen bonding of the cross-linked base pairs than do the present results. We are re-evaluating the structures of the reduced cross-links,[33,34] using a more robust rMD protocol that models solvation, in an effort to determine whether the perturbation of Watson−Crick hydrogen bonding is attributable to the older rMD protocols. Preliminary results indicate that this is the case, and that the thermodynamic destabilization of the helix induced by the reduced cross-link in the 5′-XpC-3′ sequence probably results from disruptions to base stacking interactions at the cross-link site.

Crotonaldehyde-Derived DNA Interstrand Cross-Links. The α-methyl group of the crotonaldehyde lesion can assume either the (*R*) or (*S*) configuration. In this 5′-CpG-3′ sequence the crotonaldehyde-derived 1,N^2-dG adduct with the (*R*) configuration of the α-methyl group induces DNA interstrand cross-links more efficiently than does the adduct with the (*S*) configuration of the α-methyl group. The (*R*) configuration of the α-methyl group orients the reactive aldehyde proximal to the N^2-dG cross-linking site in the complementary strand, and moreover, the resulting carbinolamine cross-link results in less structural perturbation to the DNA duplex.[28,35]

The stereochemistry of the carbinolamine carbon of the native carbinolamine cross-links is not available. The orientations of the stereoisomeric α-methyltrimethylene tethers of the reduced analogues are different.[35] For both, the steric interaction of the methyl group is minimized by the anti conformation of the methyl group with respect to C^{γ}. The orientation of the (*S*)-α-methyltrimethylene tether also reduces the steric interference of the α-methyl group with the neighbor A^8•T^{17} base pair. Extrapolating this structural information to the native cross-link suggests that the orientation of the (*R*) stereochemistry of the carbinolamine would not be positioned to form the same hydrogen bond with C^{20} O^2 at the 5′-neighbor base pair as presently observed for the acrolein-derived 1,N^2-dG exocyclic adduct.[35] Instead, formation of a hydrogen bond to C^{20} O^2 by the (*R*)-γ-hydroxytrimethylene linkage arising from the crotonaldehyde-derived (*R*)-α-methyltrimethylene tether would require reorientation of the α-CH_3 group and C^{γ} into the gauche conformation, which would be predicted to be less stable than the conformation of the (*R*)-γ-hydroxytrimethylene tether induced by acrolein-derived 1,N^2-dG adduct. This might explain, in part, why the crotonaldehyde-derived 1,N^2-dG lesion having the (*R*) configuration of the α-methyl group ultimately produces less of the interstrand cross-links in the 5′-CpG-3′ sequence than does the acrolein-derived 1,N^2-dG adduct.[5]

Summary

When placed opposite deoxycytosine in the 5′-CpG-3′ duplex, the acrolein-derived exocyclic 1,N^2-dG adduct induces stereoisomeric carbinolamine interstrand cross-links. The (*R*) configuration of the carbinolamine linkage is favored. The formation of a hydrogen bond between the hydroxyl group and C^{20} O^2 located in the 5′-neighboring base pair G^5•C^{20} may, in part, explain the stereochemical preference for the formation of the (*R*)-γ-hydroxytrimethylene linkage and its thermal stability in duplex DNA. The cross-link causes minimal structural perturbations to the DNA duplex and allows maintenance of Watson−Crick hydrogen bonding and base stacking at the tandem cross-linked base pairs.

Experimental Section

Materials. The oligodeoxynucleotide 5′-d(GGACTCGCTAGC)-3′ was synthesized and purified by anion-exchange chromatography by the Midland Certified Reagent Co. (Midland, TX). The G^{19} N^2 ^{15}N-labeled 5′-d(GGACTCGCTAGC)-3′ and the oligodeoxynucleotides containing the acrolein-derived exocyclic 1,N^2-dG adduct in the dodecamer 5′-d(GCTAGCXAGTCC)-3′ (X = 1,N^2-dG adduct **1**, whether N^2 ^{15}N-labeled or not) were synthesized, purified, and characterized as reported.[29,47] The purities of the oligodeoxynucleotides were assessed by capillary gel electrophoresis, high-performance liquid chromatography (HPLC), and matrix-assisted laser desorption/ionization time-of-flight (MALDI-TOF) mass spectroscopy. Oligodeoxynucleotides were desalted by chromatography on Sephadex G-25. The stereoisomeric carbinolamine interstrand cross-links were prepared at pH 7.0 at 37 °C, as reported.[5] Reaction was monitored by ^{15}N HSQC experiments.

NMR. Samples for the NMR experiments were at 1.0 mM strand concentration. Samples for the nonexchangeable protons were dissolved in 280 μL of a buffer containing 10 mM NaH_2PO_4, 100 mM NaCl, 50 μM Na_2EDTA (pH 7.0). They were exchanged with D_2O and suspended in 280 μL of 99.996% D_2O. The pH was adjusted to 7.0 with dilute DCl or NaOD solutions. Samples for the observation of exchangeable protons were dissolved in 280 μL of 10 mM NaH_2PO_4, 100 mM NaCl, 50 μM EDTA, (pH 7.0) containing 9:1 H_2O/D_2O (v/v), and the pH was adjusted to 7.0. ^{31}P experiments were carried out on a Bruker Avance 600 spectrometer. Other NMR experiments were performed on a Bruker Avance 500 spectrometer with a cryogenic probe (Bruker Instruments). The temperature was 25 °C for observation of the nonexchangeable protons and 5 °C for observation of the exchangeable protons. Chemical shifts for ^{1}H were referenced to water, and chemical shifts for ^{15}N and ^{31}P were referenced indirectly. Data were processed using FELIX 2000 (Accelrys Inc.). For all NMR experiments, a relaxation delay of 1.5 s was used. Two-dimensional homonuclear NMR spectra were recorded with 512 real data in the t2 dimension and 2048 real data in the t1 dimension. NOESY spectra were zero-filled during processing to create a matrix of 1024 × 1024 real points; other spectra were zero-filled to create a matrix of 1024 × 512 real points. For assignment of exchangeable protons, NOESY experiments used the WATERGATE sequence.[48] The mixing time was 250 ms. For assignment of nonexchangeable protons and the derivation of distance restraints, NOESY experiments used TPPI quadrature detection, and a mixing time of 250 ms was used. Two-dimensional (2D) ^{15}N NOESY-HSQC pulse programs were modified from corresponding 3D pulse program[49,50] with 128 points centered at 81 ppm. The water signal was suppressed with the WATERGATE method. The mixing time was 250 ms. The spectrum was recorded with 512 real data in the t2 dimension and 2048 real data in the t1 dimension and was zero-filled during process to create a 1024 × 512 matrix.

Experimental Restraints. NOE-derived distance restraints used for the refinement of the (*R*)-γ-hydroxytrimethylene structure were calculated from NOE cross-peak volumes in the ^{15}N NOESY-HSQC

(47) Nechev, L. V.; Harris, C. M.; Harris, T. M. *Chem. Res. Toxicol.* **2000**, *13*, 421–429.
(48) Piotto, M.; Saudek, V.; Sklenar, V. *J. Biomol. NMR* **1992**, *2*, 661–665.
(49) Mori, S.; Abeygunawardana, C.; Johnson, M.; van Zul, P. C. M. *J. Magn. Reson., Ser. B* **1995**, *108*, 94–98.
(50) Talluri, S.; Wagner, G. *J. Magn. Reson., Ser. B* **1996**, *112*, 200–205.

spectra using MARDIGRAS v3.2.[51,52] Isotropic correlation times 2, 3, and 4 ns were used. The relaxation time for the analyses was 1.5 s. The volume error was one-half the volume of the smallest peak. Volumes were normalized based on all the peak intensities. The RANDMARDI algorithm carried out 50 iterations for each set of data, randomizing peak volumes within limits specified by the input noise level.[53] The distances were averaged. The standard deviation in a particular distance served as the error bond for the distance. Empirical restraints preserving Watson−Crick hydrogen bonding and preventing propeller twisting between base pairs were used.[54] The backbone and sugar pucker torsion angle restraints were also derived using empirical data derived from B-DNA.[55]

Structural Refinement of the (*R*)-γ-Hydroxytrimethylene Cross-Link. Molecular dynamics simulations used the AMBER force field (Vol. 9, parm99 force field).[56] Partial charges of the carbinolamine linkage were obtained by density functional theory (DFT) calculation at B3LYP/6-31G* level with Gaussian 03.[57] Starting structures were constructed from A- and B-type DNA using Insight II. The duplexes were energy minimized by conjugate gradients for 1000 iterations without experimental and empirical restraints. Molecular dynamics simulations were carried out in explicit water using the particle mesh Ewald (PME) method. DNA duplexes were placed in a 10 Å cubic TIP3P water box. Twenty-two Na^+ ions were added to neutralize the DNA interstrand cross-link. The cutoff radius for nonbonding interactions was 10 Å. The restraint energy function contained terms describing distance and torsion angle restraints, both in the form of square well potentials. Bond lengths involving hydrogens were fixed with the SHAKE algorithm.[58]

First, a 1000-step energy minimization was performed with an integrator time of 1 fs with the heavy atoms of the cross-link restrained. A 10,000-iteration simulation was carried out with constant volume at 300 K. The heavy atoms of the cross-link were restrained. Then, molecular dynamics simulation at constant pressure was performed at 300 K for 8 ns with an integrator time of 1 fs. Experimental and empirical distance and torsion angle restraints with force constants of 32.0 $kcal \cdot mol^{-1} \cdot Å^{-1}$ were applied. One trajectory was saved in each 1000-iteration during simulation. The trajectories after reaching simulation equilibrium were averaged. The mean structures were filtered out from water box and energy-minimized for 250 iterations without experimental and empirical restraints.

The PTRAJ program from AMBER 9 package was used to analyze the trajectories. The rmsd values of the trajectories were referenced to the starting structures. A distance of less than 3.5 Å, and an angle of greater than 120° between the potential hydrogen donor and acceptor, were used as criteria for hydrogen bond formation. The backbone conformation of the average structure was analyzed with the program 3DNA.[59]

Structural Refinement of the (*S*)-γ-Hydroxytrimethylene Cross-Link. Similar molecular dynamics simulations were performed to refine the structure of the (*S*)-γ-hydroxytrimethylene cross-link. Because this was the minor species in solution, it was not possible to obtain experimental NOEs, and thus molecular dynamics simulations were carried out without experimental distance restraints.

Acknowledgment. Dr. Markus Voehler assisted with NMR experiments. This work was supported by NIH Grant PO1 ES-05355 (C.J.R., T.M.H., and M.P.S.).

Supporting Information Available: Table S1, NOEs used in the rMD simulations and the corresponding atom distances in the average refined structure, complete refs 56 and 57. This material is available free of charge via the Internet at http://pubs.acs.org.

JA809543J

(51) Borgias, B. A.; James, T. L. *J. Magn. Reson.* **1990**, *87*, 475–487.
(52) Liu, H.; Tonelli, M.; James, T. L. *J. Magn. Reson., Ser. B* **1996**, *111*, 85–89.
(53) Liu, H.; Spielmann, H. P.; Ulyanov, N. B.; Wemmer, D. E.; James, T. L. *J. Biomol. NMR* **1995**, *6*, 390–402.
(54) Kouchakdjian, M.; Marinelli, E.; Gao, X.; Johnson, F.; Grollman, A.; Patel, D. *Biochemistry* **1989**, *28*, 5647–5657.
(55) Blackburn, G. M.; Gait, M. J. *Nucleic Acids in Chemistry and Biology*; Oxford University Press: New York, 1996.
(56) Case, D. A.; et al. AMBER 9; University of California, San Francisco: San Francisco, CA, 2006.
(57) Frisch, M. J.; et al. Gaussian 03; Gaussian, Inc.: Wallingford, CT, 2004.
(58) Ryckaert, J.-P.; Ciccotti, G.; Berendsen, H. J. C. *J. Comput. Phys.* **1977**, *23*, 327–341.
(59) Lu, X.-J.; Olson, W. K. *Nucleic Acids Res.* **2003**, *31*, 5108–5121.